



## Mathematical Simulation of SO<sub>2</sub> Emissions from a Fluidized Bed

O. O. OLAYEBI<sup>1</sup>, M.A. AZEEZ<sup>2</sup> and A. S. OLUFEMI<sup>3\*</sup>

<sup>1</sup>Department of Chemical Engineering, Federal University of Petroleum Resources, Effurun, Delta State, Nigeria.

<sup>2</sup>Department of Chemistry, State University of Ekiti, Ado-Ekiti, Ekiti State, Nigeria.

<sup>3</sup>Department of Chemical/Petroleum Engineering, Niger Delta University, Wilberforce Island, Bayelsa State, Nigeria.

\*Corresponding author: A. S. OLUFEMI, E-mail: [adestanford.olufemi@gmail.com](mailto:adestanford.olufemi@gmail.com)

Received: April 25, 2017, Accepted: May 30, 2017, Published: May 30, 2017.

### ABSTRACT:

In this paper a mathematical model and experimental techniques to describe the combustion behavior of coal and biomass in a fluidized bed is presented. This study is of practical interest due to its significant involvement in heating systems and power plant operations. One dimensional Mathematical model is being developed to predict the SO<sub>2</sub> emissions under different operating conditions like bed temperature, Ca/S molar ratio, solids circulation rate, excess air ratio and secondary to primary air ratio from a burning coal and biomass. For the fast section of the bed, momentum and energy balance equations are used to predict temperature and velocity profiles for gas and particles. The model performs mass balances for the chemical gas species (O<sub>2</sub>, H<sub>2</sub>O, CO<sub>2</sub>, CO and SO<sub>2</sub>) with consideration on the last being given for retention by limestone particles. A bubbling bed model is considered to simulate the bottom of the fluidized bed. These parameters are varied to validate the model and encouraging correlation is found between the experimental values and model predictions. The model is applied to typical conditions of a boiler and the results show the expected trends.

**Keywords:** *fluidized-bed, mathematical-model, SO<sub>2</sub>-Emission,*

### INTRODUCTION

Circulating fluidized bed combustors (CFBCs) are considered as an improvement over the old method of bubbling bed. They exhibit several advantages that include fuel flexibility, broad turndown ratio, high combustion efficiency, low NO<sub>x</sub> emissions and high sulfur capture efficiency over conventional coal combustion methods, especially when carrying out operations with fine solids at very high velocities and also when high sulfur coal is used. In this way, became a significant topic of research. The experimental design of boiler furnaces practiced for many years promoted studies to understand the processes occurring in such equipment. These days, because of prohibitive pollution regulation, there are some significant uncertainties in predicting their performance in large-scale systems. This necessitate the introduction of high performing computers for research programs. Technical knowledge about design and operation of CFBC is widely available for pilot plant and large scale units [1]. Investigations on high-velocity fluidization have been conducted by many investigators [2-4]. These models permit the identification of the fluidized bed structure, with a denser zone at the bottom and a fast bed above, with higher particle absorptions in the wall region.

However, little has been done in the field of mathematical modeling and simulation of combustion in CFBCs. This might be attributed to the fact that the combustion process occurring in a CFBC involves complex phenomena including chemical reactions, heat and mass transfer, particle size reduction due to combustion, attrition, fragmentation and other mechanisms, gas and solid flow structure.

Weiss *et al.* [5] introduced a CFBC model by dividing it into 11 blocks, each corresponding to a CSTR reactor for both gas and solid phase. Five of these blocks related to the CFBC riser,

however, no details are given about the solids distribution in the reactor and no special treatment is given to the bottom region., CFBC model was developed by Basu *et al.* [6], in which a plug flow regime for both the gas and solids is assumed. Lee and Hypanen [7], also presented a CFBC model which studied the riser as a plug flow reactor for the gas phase and a CSTR reactor for the solid phase. The model also considers the feed particle size distribution and the attrition phenomena. Using a lumped-modeling approach, Arena *et al.* [8], introduced the means for predictive calculation by dividing the CFBC riser into four blocks, each corresponding to a separate reactor. Three of these blocks related to the CFBC riser.

Kunni and Levenspiel [9], developed a model for the hydrodynamics which considers three different phases, (dilute particles entrained, ascending and descending clusters), with mass transfer between them. The key parameter in their model is the decay constant for the fall off of bulk density of solids with height in the freeboard. Berruti and Kalogerakis [10], modelled the fast bed hydrodynamics using a core-annulus theory which is applied to small diameter risers ( $d < 0.3$  m) used in catalytic processes.

Classification of different types of model based on complexity as global models, one dimensional model, multi-dimensional model (computational fluid dynamics) and scaling and expert systems were done by Hannes [11]. Hartleben [12], presented the first model for atmospheric and pressurized circulating fluidized beds in which an empirical approach was used for the fluid dynamics and particle size distribution.

Different models had been developed to estimate the concentrations of CO, CO<sub>2</sub>, and NO<sub>x</sub> [13] and to calculate the oxygen concentration, carbon fraction and char size distribution [14].

The objective of the present study is to model the CFB rig for the

estimation of SO<sub>2</sub> emissions under different operating conditions and compare the model values to the experimental values. The values of bed temperature, Ca/S molar ratio, solids circulation rate, excess air ratio and secondary to primary air were varied to validate the model.

## MATERIAL AND METHODS

### Experimental Setup

CFB combustor used in this investigation is shown in Figure 1. The system comprised of a riser of 0.152 m i.d. and 6.2 m height, two high efficiency cyclones in series, an external heat exchanger (EHE) and an L-valve. The coal and wheat straw were supplied from gravimetric hoppers with screw feeders coupled with variable speed motors.

More detail regarding the experimental setup and operation can be seen elsewhere [15]. Silica sand, having sauter mean diameter (SMD) of 125 μm and particle density of 2500 kg/m<sup>3</sup> is used as the circulating bed material. Wood waste (SMD = 0.85 mm) and Nigerian subbituminous coal (SMD = 0.49 mm) are used as the fuel in this study.

Analyses and heating values of the feed materials are given in Table 1. Reported values are the mean of three values taken as per ASTM standards. The concentrations of SO<sub>2</sub>, NO<sub>x</sub> and CO in flue gas are measured by on line gas analyzers. Dry flue gas is also sampled in Teflon bags to analyze in gas chromatograph (Perkin Elmer Auto system GC Arnel). All reported values are corrected

to 6 % O<sub>2</sub> in the flue gas. Limestone (98.6 % CaCO<sub>3</sub>, SMD= 129 μm and ρ = 2730 kg/m<sup>3</sup>) is also added as the sulfur capture sorbent through feeder.

Coal combustion model developed by Hannes [11] was used as a base model in this study. Effect of bed temperature, Ca/S molar ratio, solids circulation rate and secondary to primary air ratio, on the sulphur retention was predicted from the mathematical model at different blend ratios. Model results have been compared with the experimental results to see the reliability and synergy effect.

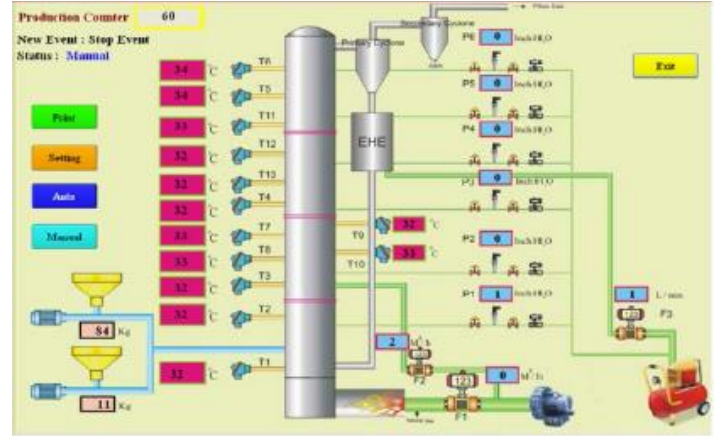


Figure 1. Visual view of CFB rig.

Table 1. Analysis of coal and wood-waste

	Proximate Analysis			Elemental Analysis					GCV
	VM	FC	Ash	C	H	N	S	O	MJ/kg
Salt range Coal (%) <sup>db</sup>	38.60	43.90	17.50	68.90	9.8	0.56	4.2	16.54	25.55
Wood waste (%) <sup>db</sup>	73.12	19.98	6.90	47.50	7.35	1.20	-	43.95	18.20

db = dry basis

### Modelling Approach

All main reactions were assumed to take place in the riser as in the return leg, temperature dropped and the availability of oxygen was small. For the use of matrix solver, it was reasonable to continue the annular phase into the dense bed, so that bed and freeboard could be solve together and continuously. The lateral mixing between core and annulus in the dense bed region was set high enough to equalize both phases to a common dense bed. All balances were setup by setting the time dependent term to zero to achieve steady state conditions. The gas flows were split using the values from the pre-calculations of the bubble holdup and the annulus width. The gas flow was balanced as molar flow. Changes caused by reactions which were not equimolar were assumed to have no influence on fluidization. The balanced flows were the convective flow in each phase (cor, ann, bub), cross flows from core to annulus (cor-ann), core to bubble (cor-bub) and vice versa, and mixing flows between the phases (corannx, corbubx).

### Mass and Energy Balances

For mass balance, gaseous flows were balanced based on the following differential equation:

$$\frac{dn_g}{dt} = u_g \frac{\partial n_g}{\partial z} + \Psi_{source} + \Psi_{exchange} \quad (1)$$

An overall population balance was done to get the size distribution of the bed inventory. Then size classes (*i*) of the different materials (*m*), (coal, limestone, sand and ash) were balanced separately for each cell (*L*). The following differential equation was discretized for each phase (cr, anl) considering size, materials and location (cell) of the solids.

$$\frac{dm_s}{dt} = u_s \frac{dm_s}{dz} + \Psi_{s,source} \quad (2)$$

In the lowest cell of the riser, all annular material had to be returned to the core to conserve the mass balance. Reactive species such as CaO and the combustibles in the coal were modelled as solid fractions. For better system solubility, the mass flow of the particles was kept constant, only the species fractions might vary. The fluidization pattern and char holdup was assumed not to be influenced by these changes. Coal mass was treated as virtual fraction, it did not influence the flow pattern but delivered the source terms for evaporated water and released volatiles. Only the ash residue in the char was balanced in the size distribution calculation. The fixed carbon was treated as ash load. The fraction balance was based on the following equation:

$$\frac{\partial(m_s \cdot x)}{\partial t} = u_s \frac{d(m_s \cdot x)}{dz} + \Psi_{s,source} + kM_s x \quad (3)$$

Where the last term represents the release or reaction influence. “*k*” is a release or reaction constant depending on local gas concentrations and temperature. Drying and de-volatilization are time dependent processes. The time dependent fraction was determined and averaged for each cell (*L*) and class (*i*) as under:

$$x_{avg}(i, L) = \int_0^{\tau} \frac{\partial x(i, L, t)}{\partial t} dt \quad (4)$$

All these equations were written as first order equations for concentrations. The solution of the concentration equations is done analogue to the enthalpy balances.

The enthalpy balance delivered the average cell temperature. Enthalpy balance was based on the convective flows of gas and solids, changes in formation enthalpies due to reactions and the

heat transfer to the walls. Following differential equation was used for the energy balance.

$$\left(n_g C_{pg} + m_s C_{ps}\right) \frac{dT}{dt} = \left(u_g n_g C_{pg} + u_s m_s C_{ps}\right) \frac{dT}{dz} + \Psi_{\text{reac}} + Q_{\text{heatexch}} \quad (5)$$

### Sulphation Model

Lime stone is added into the CFB combustor to capture SO<sub>2</sub> directly. It is very tough to model the self-desulphurization of the coal, done by the mineral and metallic fractions in coal. The self-desulphurization of the coal is not explicitly modelled, however it can be taken into account by reducing the sulphur content in the coal by the amount of available calcium [11]. The capture of sulphur with limestone particles undergoes three principle reaction steps which are as follows:

1) calcination:



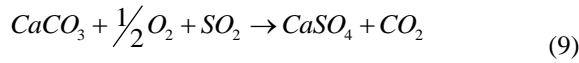
2) oxidation:



3) sulphation:



Overall reaction can be written as under:



Thus, the sulphur capture capability strongly depends on the residence time, the fragmentation behaviour, and the pore structure of the sorbent. Calcium-sulphur compounds do not only exist as CaSO<sub>4</sub> but may also exist as CaS, depending upon oxidizing or reducing boundary conditions, respectively. Since in fluidized beds the residence times of the particles are high and the sulphation reaction is slow, particle tracking is nearly impossible to distinguish in reducing and oxidizing zones as they mix within short times. Therefore, only the oxidizing conditions are considered in the following model.

During the calcination, the equilibrium between CaCO<sub>3</sub> and CaO is dependent on the partial pressure of CO<sub>2</sub> in the surrounding gas, and on temperature. Baker [16] stated, that this equilibrium pressure can be written as:

$$pCO_{2,eq} = 1.2 \times 10^7 \exp\left(-\frac{1924K}{T}\right) (\text{bar}) \quad (10)$$

For a given partial pressure of CO<sub>2</sub>, calcination will only take place above the corresponding temperature. Dennis and Fieldes

[17] have calculated the calcination time  $t_{\text{calc}}$  by:

$$t_{\text{calc}} = \frac{R_{p,0} M_{CaCO_3}}{k_0 (pCO_{2,eq} - pCO_2 - pX_{CO_2})} \quad (11)$$

With  $k_0 = 207$  (mol/bar·m<sup>2</sup>·s) and an empirical variable describing a constant molar fraction of CO<sub>2</sub> which is 0.065 at 825 °C, 0.1 at 875 °C and 0.17 at 925 °C.

For a kinetically controlled shrinking-core model, Kunii and Levenspiel [18] correlate the calcination time with the core radius and the conversion degree as:

$$\frac{t}{t_{\text{calc}}} \left(1 - \frac{R_{\text{core}}}{R_{p,0}}\right) = 1 - (1 - x_{\text{calc}})^{0.33} \quad (12)$$

The combination with residence time of the particles is done with a residence time distribution:

$$E(t) = \frac{1}{\tau} \exp\left(-\frac{t}{\tau}\right) \quad (13)$$

Where the average residence time is the quotient of limestone mass in the furnace and limestone feed flow. The average calcination degree is

$$1 - x_{\text{calc}} = \int_0^{t_{\text{calc}}} \left(1 - \frac{t}{t_{\text{calc}}}\right)^3 \frac{\exp\left(-\frac{t}{\tau}\right)}{t} dt \quad (14)$$

On integration

$$x_{\text{calc}} = 3 \left(\frac{\tau}{t_{\text{calc}}}\right) - 6 \left(\frac{\tau}{t_{\text{calc}}}\right)^2 + 6 \left(\frac{\tau}{t_{\text{calc}}}\right)^3 \left(1 - \exp\left(-\frac{t_{\text{calc}}}{\tau}\right)\right) \quad (15)$$

During calcination, the released CO<sub>2</sub> leaves the limestone with No. of pores which increases the inner surface area and subsequently sulphation reactions. Shrinking core model was used for the sulphation reaction due to its validity [19] as shrinking core models consider the “particle as a porous sphere”, surrounded by a thin gas layer and consisting of an unreacted core in the particle surrounded by a shell of already sulphated material [18]. The radius of the unreacted core shrinks with time enlarging the shell which causes a higher diffusion resistance for the penetrating gases [20, 21].

Gas-solid reaction model, describing the reactions taking place at the individual particles is combined with the hydrodynamic model delivering the particle flow rates and concentrations. This model has differentials in time and radius, which are to be solved properly. So Wolff approach is implemented into the sulphation model, based on an analytical way to solve the radius dependent integral, so that only a forward integration in time remains [21]. The basic balance is the deliverance of the reactants by diffusion and the reaction at the surface of the unreacted core [22]:

$$4\pi r^2 \left(D_{SO_2} \frac{dC_{SO_2}}{dr} + D_{SO_3} \frac{dC_{SO_3}}{dr}\right) = 4\pi r k_{\text{sulf}} \cdot C_{SO_3} \quad (16)$$

Where the equilibrium between SO<sub>2</sub> and SO<sub>3</sub> can be expressed by:

$$C_{SO_3} = K_0 \cdot C_{SO_2} \sqrt{C_{O_2}} \quad \text{with} \quad K_0 = 0.154 \sqrt{\frac{m^3}{mol}} \quad (17)$$

The reaction rate at the core surface can be stated as [11]:

$$\frac{dn_{CAO}}{dt} = -\gamma \cdot k_{\text{sulf}} \cdot 4\pi r^2 \cdot K_0 \cdot \sqrt{C_{O_2} \cdot C_{SO_2r}} \quad (18)$$

Equation (18) can be solved as follows:

$$n_{CAO} = \frac{4}{3} \pi r^3 \cdot \frac{C_{O_2} \rho_{\text{lime}}}{M_{CaCO_3}} \cdot x_{\text{calc}} \cdot x_{CaCO_3} \quad (19)$$

Integration over the reacted shell and the gas film leads to the concentration of SO<sub>2</sub> on the core surface dependent on the bulk SO<sub>2</sub> concentration.

$$C_{SO_2r} = \frac{C_{SO_2, R+\delta}}{1 + K_0 \cdot \sqrt{C_{O_2}} \cdot k_{\text{sulf}} \cdot r^2 (f_{\text{film}} + f_{\text{shell}})} \quad (20)$$

Substitution back into Equation (16) and rewriting yields:

$$\frac{dr}{dt} = \frac{\gamma \cdot \frac{C_{SO_2, R+\delta}}{\rho_{\text{lime}} \cdot x_{\text{calc}} \cdot x_{CaCO_3}}}{\frac{1}{k_s \cdot k_0 \cdot \sqrt{C_{O_2}}} + r^2 (f(D_{\text{film}}) + f(D_{\text{shell}}))} \quad (21)$$

From the integration of left side of Equation (16) over the gas shell and over the reacted shell, the diffusion functions  $f_{\text{film}}$  and  $f_{\text{shell}}$  can be derived [23], which are:

$$f_{film} = \frac{1}{D_{SO_2, film} + D_{SO_3, film} K_0 \sqrt{C_{O_2}}} \left( \frac{1}{R} - \frac{1}{R + \delta} \right) \quad (22)$$

$$f_{shell} = \frac{1}{D_{SO_2, shell} + D_{SO_3, shell} K_0 \sqrt{C_{O_2}}} \left( \frac{1}{r} - \frac{1}{R} \right) \quad (23)$$

The conversion  $\alpha_{lime}$  can be understood as reacted volume fraction of the particle

$$\alpha_{lime}(t) = 1 - \frac{r^3(t)}{R^3} \quad (24)$$

Averaged conversion is approached with a residence time distribution function [19],

$$\alpha_{lime} = \int_0^{\infty} \alpha_{lime}(t) E(t) dt$$

$$E(t) = \frac{1}{\tau} \exp\left(-\frac{t}{\tau}\right)$$

where  $\tau$  is the residence time. (25)

Above equation can be solved analytically using a substitution of Equation (24) into Equation (21).

$$\frac{1}{f(\alpha_{lime})} = \frac{1}{3\tau C_1} \left( C_2 (1 - \alpha_{lime})^{-\frac{2}{3}} + C_3 (1 - \alpha_{lime})^{-\frac{1}{3}} + (C_4 - C_3) \right) \quad (26)$$

With values of  $C_1$ ,  $C_2$ ,  $C_3$  and  $C_4$  as

$$C_1 = \gamma \frac{C_{SO_2, R+\delta}}{\frac{\rho_{lime}}{M_{CaCO_3}} \cdot x_{calc} \cdot x_{CaCO_3}}, \quad C_2 = \frac{R}{k_{sulf} \cdot k_0 \cdot \sqrt{C_{O_2}}}$$

$$C_3 = \frac{R^2}{D_{SO_2, shell}}, \quad C_4 = \frac{R^3}{D_{SO_2, film}} \left( \frac{1}{R} - \frac{1}{R + \delta} \right)$$

Final integration of Equation (26) is,

$$\int_0^{\alpha_{lime, max}} \frac{1}{f(\alpha_{lime})} = \frac{1}{\tau C_1} \left( C_2 \left( 1 - (1 - \alpha_{lime})^{\frac{1}{3}} \right) + \frac{C_3}{2} \left( 1 - (1 - \alpha_{lime})^{\frac{2}{3}} \right) + \frac{C_4 - C_3}{3} \alpha_{lime} \right) \quad (27)$$

This equation is replaced with residence time distribution function and numerically integrated using a modified Euler method. The function has as very steep gradient for very small values of  $\alpha_{lime}$  and flattens with increasing values.

The diffusion coefficients consist of the Knudsen diffusion effects in the pores and the diffusion of a binary mixture of gases [24].

In the gas film, only binary diffusion occurs [25], so it can be assumed that  $D_{SO_2, film} = D_{mix}$ . In the shell, i.e. in the pores, Knudsen and gas diffusion must be considered [22]:

$$D_{SO_2, shell} = D_{pore} = \frac{\rho_{lime} \cdot V_{pore}}{\tau_{tort}} \left( \frac{1}{D_{knud}} + \frac{1}{D_{mix}} \right) \quad (28)$$

The calculation of the thickness of the gas film layer  $\delta$  is estimated by the mass transport coefficient  $k_{SO_2}$  [26]:

$$\delta = \frac{1}{\frac{k_{SO_2, film}}{D_{SO_2, shell}} + \frac{1}{R}} \quad (29)$$

where

$$k_{SO_2} = \frac{St \cdot u_g}{\varepsilon_g}, \quad St = 0.81 \cdot Re_p^{-0.5} \cdot Sc^{-0.66}$$

$$Sc = \frac{\mu_g}{\rho_g \cdot D_{mix}}, \quad Re_p = \frac{\rho_g \cdot u_g \cdot d_p}{\mu_g}$$

So the reaction rates and concentrations were calculated and following parameters were used in the model,

$K_0 = 0.154$  ( $SO_4/SO_3$  equilibrium constant) [27];

$\tau_{tort} = 3$  (tortuosity factor) [28];

$\alpha_{max} = 0.5$  (maximum conversion degree) [18];

$k_{sulf} = 0.15$  (sulphation constant m/s) [28].

Since the residence time of limestone particles and their sulphation takes place over hours, while gas residence time is in seconds, the sorbent is balanced as a homogenous phase. This is done by considering fragmentation and attrition of the sorbent which enlarges the available reactive surface. The conversion rate is calculated with an averaged  $SO_2$  bulk concentration. The gas reaction is calculated depending on local holdup of sorbent in the riser. Weighing the local  $SO_2$  concentrations with the local holdup of sorbent provides the average gas concentration for the calculation to determine the conversion of the sorbent. The steady state sorbent conversion and gas concentration is established during the overall mass balance in the program.

To see the synergy effects and validate the model, its predictions were compared with the experimental data taken from the CFB test rig.

## RESULTS AND DISCUSSION

Typical results obtained through the model and experimental studies are shown from Figures 2-6. There is a good agreement between the model predictions and the experimental results in accordance with the synergy effects of coal and biomass combustion, on emissions of  $SO_2$ . Model was run with a series of input values but reported values are, for bed temperature, excess air factor, secondary to primary air ratio, solid circulation rate and Ca/S molar ratio, for 5 %, 10 % and 20 % blends of wheat straw with coal on weight basis.

It was believed that an increase in bed temperature can accelerate the calcination reaction resulting in low  $SO_2$  concentration. High bed temperature also resulted in low CO concentrations which adversely affect the decompositions reactions of  $CaSO_4$ . Model predictions were in agreement when compared to the experimental values for different bed temperatures as shown in Figure 2. At higher temperature, higher conversion of lime stone and higher reaction rates of sulphation reactions were depicted in model as experimentally found to be happening in the furnace.

Agreement between model predictions and experimental results were found to be very encouraging for the effect of Ca/S molar ratio on  $SO_2$  emission as shown in Figure 3. Predicted values are more close to the experimental values for Ca/S molar ratios of 2 compared to that of 3. Model was also producing the reliable values at low wheat straw ratio in coal. Deviation at high wheat straw ratio in coal blend might be due to the different devolatilization kinetics of biomass compared to the coal.

Effect of variation of excess air factor on the  $SO_2$  emission, predicted by the model is shown in Figure 4. Model has shown the correct tendencies for different values of excess air factor at different blends of biomass with coal on weight basis, although the model predictions were very slightly higher than the experimental ones. As incorporated in the model, increased concentrations of oxygen would facilitate the sulphation reaction, resulting in low

SO<sub>2</sub> emission. With an excess air factor of 1.20, reaction rate of sulphation increased due to higher oxygen concentration in the riser. Based on the same scenario, SO<sub>2</sub> emission decreased in the actual experimental work.

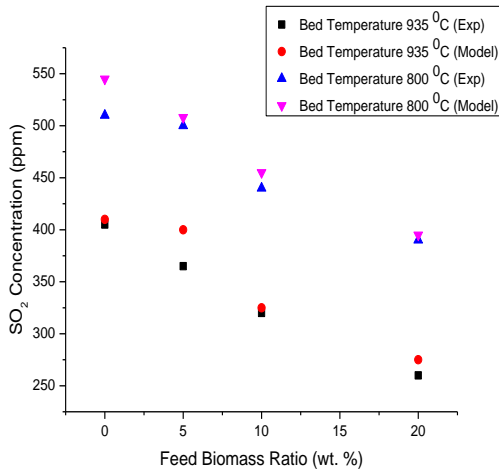


Figure 2. Bed temperature vs. SO<sub>2</sub> concentration, experimental results and model predictions.

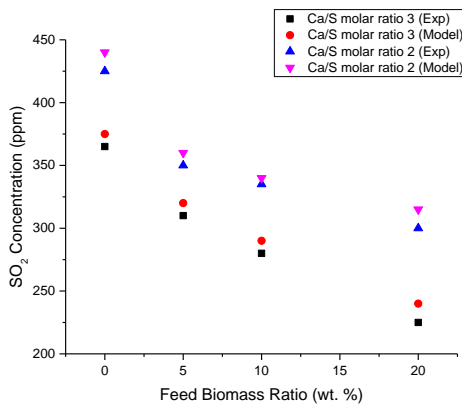


Figure 3. Ca/S molar ratio vs. SO<sub>2</sub> concentration, experimental results and model predictions.

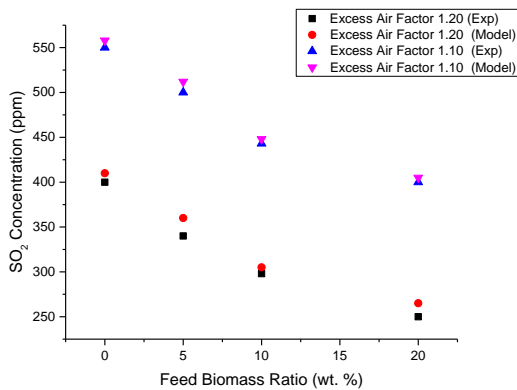


Figure 4. Excess air factor vs. SO<sub>2</sub> concentration, experimental results and model predictions.

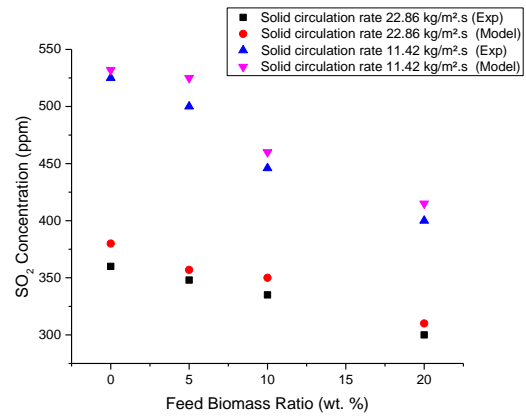


Figure 5. Solids circulation rate vs. SO<sub>2</sub> concentration, experimental results and model predictions.

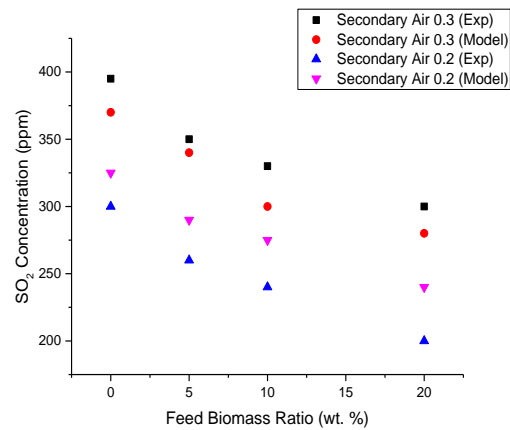


Figure 6. Secondary air to primary air ratio vs. SO<sub>2</sub> concentration, experimental results and model predictions.

Experimental and model results related to the effect of solids circulation rate on SO<sub>2</sub> emissions have been compared and reported in Figure 5. Model predictions have given the good relation in response to the variation in solid circulation rate, however minor deviations were also observed. At the value of 22.86 kg/m<sup>2</sup>.s, the error was small and model has given the good predictions especially at higher wheat straw ratio.

In Figure 6, model predictions of effect of secondary to primary air ratio on SO<sub>2</sub> emission have been compared with the experimental results. As clear from the results, model was unable to produce good correlation for the variation in secondary to primary air ratio for the SO<sub>2</sub> emission. Model predictions have given a positive error for lower secondary to primary air ratio while a negative error was observed for the higher values of secondary to primary air ratio. This might be due to the complex hydrodynamics inside the riser produced after the secondary air injection which could not be accounted in the present correlations used for the hydrodynamic modelling of the riser. As by the injection of secondary air, temperature of that region will be low and more oxidizing conditions would be made available making a precarious region regarding the model. Especially variation in the secondary to primary air ratio produced the undesired effect on the hydrodynamics of the riser that ultimately affected the SO<sub>2</sub> concentration.

## CONCLUSION

A fluidized bed model for the steady state combustion and sulphation in a CFB was used to predict the SO<sub>2</sub> concentrations in

the exit flue gases. It was based on the shrinking core model. Agreement between model prediction and experimental results was found encouraging for the parameters like bed temperature, fluidizing air velocity, excess air ratio and solids circulation rate. However for secondary to primary air ratio, some short comings in the model were observed.

## REFERENCES

- Sotudeh-Gharebaagh, R., et al., Simulation of circulating fluidized bed reactors using ASPEN PLUS. *Fuel*, 1998. 77(4): p. 327-337.
- Yerushalmi, J. and A. Avidan, High velocity fluidization. *Fluidization*, 1985: p. 225-291.
- Kwauk, M., et al., Fast fluidization at ICM. *Circulating Fluidised Bed Technology*, 1987: p. 33-45.
- Rhodes, M. and D. Geldart, A model for the circulating fluidized bed. *Powder Technology*, 1987. 53(3): p. 155-162.
- Weiss, V., et al., Mathematical modelling of circulating fluidized bed reactors by reference to a solids decomposition reaction and coal combustion. *Chemical Engineering and Processing: Process Intensification*, 1987. 22(2): p. 79-90.
- Basu, P., A. Sett, and E. Gbordzoe, A simplified model for combustion of carbon in a circulating fluidized bed combustor. *FBC Comes Of Age*, (Ed.: JP Mustonen), ASME, 1987.
- Lee, Y. and T. Hyppanen. A coal combustion model for circulating fluidized bed boilers. in *Proceedings of the Tenth International Conference on Fluidized Bed Combustion*. 1989.
- Arena, U., et al., Hydrodynamics of circulating fluidized beds with risers of different shape and size. *Powder technology*, 1992. 70(3): p. 237-247.
- Kunii, D. and O. Levenspiel, Entrainment of solids from fluidized beds I. Hold-up of solids in the freeboard II. Operation of fast fluidized beds. *Powder Technology*, 1990. 61(2): p. 193-206.
- Berruti, F. and N. Kalogerakis, Modelling the internal flow structure of circulating fluidized beds. *The Canadian Journal of Chemical Engineering*, 1989. 67(6): p. 1010-1014.
- Hannes, J., U. Renz, and C.M. Van den Bleek, *The IEA model for circulating fluidized bed combustion*. 1995, American Society of Mechanical Engineers, New York, NY (United States).
- Hartleben, B., *Mathematische modellierung von blasenbildenden kohlewirbelschicht-feuerungsanlagen*. 1983: na.
- Lin, X. and Y. Li. A Two Phase Model for Fast Fluidized Bed Combustion. in *4th International Conference on Circulating Fluidized Beds*, Somerset. 1993.
- Halder, P. and A. Datta. Modelling of Combustion of a Char in a Circulating Fluidized Bed. in *4th International Conference on Circulating Fluidized Beds*, Somerset. 1993.
- Khurram, S., et al., Parametric Study of NO<sub>x</sub> Emissions in Circulating Fluidized Bed Combustor. *Journal of Pakistan Institute of Chemical Engineers*, 2012. 40: p. 61-68.
- Baker, E.H., The Calcium Oxide-Calcium Dioxide System in the Pressure Range 1 - 300 Atmospheres. . *Journal of Chemical Society*, 1962. 165: p. 464-470.
- Dennis, J.S. and R.B. Fieldes, Simplified Model for the Rate of Sulphation of Limestone Particles. *Chemical Engineering Research and Design*, 1986. 64: p. 279-287.
- Kunii, D. and O. Levenspiel, *Fluidization Engineering*. 2nd ed. 1991, Boston, MA: Butterworth-Heinemann.
- Hannes, J., K. Svoboda, and C. van den Bleek. Modelling of Size Distribution and Pressure Profiles in a CFBC. in *4th International Conference on Circulating Fluidized Beds*, Somerset. 1993.
- Korbee, R., Regenerative desulfurization in an interconnected fluidized bed system. 1995.
- Wolff, E., Regenerative sulfur capture in fluidized bed combustion of coal. 1991, PhD Thesis, Delft University of Technology, The Netherlands.
- Hannes, J.P., et al. Mathematical Modelling of CFBC: An Overall Modular Programming Frame Using a 1.5-Dimensional Riser Model. in *12th International Conference on Fluidized Bed Combustion* (ed. LN Rubow). 1993.
- Hannes, J.P., *Mathematical Modelling of Circulating Fluidized Bed Combustion*. 1996, Technical University Delft: Delft.
- Haider, A. and O. Levenspiel, Drag coefficient and terminal velocity of spherical and nonspherical particles. *Powder technology*, 1989. 58(1): p. 63-70.
- Hiller, R., *Mathematische Modellierung der Kohleverbrennung in einer Circrofluid-Wirbelschichtfeuerung*. 1995: Shaker.
- Mori, S. and C. Wen, Estimation of bubble diameter in gaseous fluidized beds. *AIChE Journal*, 1975. 21(1): p. 109-115.
- Hansen, P.F.B., W. Lin, and K. Dam-Johansen, *Chemical reaction conditions in a Danish 80 MW {sub th} CFB-boiler co-firing straw and coal*. 1997, American Society of Mechanical Engineers, New York, NY (United States).
- Dam-Johansen, K. and K. Østergaard, High-temperature reaction between sulphur dioxide and limestone—I. Comparison of limestones in two laboratory reactors and a pilot plant. *Chemical Engineering Science*, 1991. 46(3): p. 827-837.

**Citation:** A. S. OLUFEMI, *et al.* (2017). Mathematical Simulation of SO<sub>2</sub> Emissions from a Fluidized Bed. *J. of Computation in Biosciences and Engineering*. V3I4. DOI: 10.15297/JCLS.V3I4.04

**Copyright:** © 2017 A. S. OLUFEMI, This is an open-access article distributed under the terms of the Creative Commons Attribution License, which permits unrestricted use, distribution, and reproduction in any medium, provided the original author and source are credited.